

Article

OsMDH12: A Peroxisomal Malate Dehydrogenase Regulating Tiller Number and Salt Tolerance in Rice

Yuheng Shi ^{1,2,†}, Jiahui Feng ^{1,2,†}, Liping Wang ^{1,2,†}, Yanchen Liu ^{1,2} , Dujun He ^{1,2}, Yangyang Sun ^{1,2} , Yuehua Luo ², Cheng Jin ^{1,2}  and Yuanyuan Zhang ^{1,2,*} 

¹ School of Breeding and Multiplication (Sanya Institute of Breeding and Multiplication), Hainan University, Sanya 572025, China; shiyuheng@hainanu.edu.cn (Y.S.); fjh45797301@163.com (J.F.); 21210901000041@hainanu.edu.cn (L.W.); liuyanachen@hainanu.edu.cn (Y.L.); hdjjjaptx4869@163.com (D.H.); sunyyhn@hainanu.edu.cn (Y.S.); jincheng@hainanu.edu.cn (C.J.)

² School of Tropical Agriculture and Forestry, Hainan University, Haikou 570228, China; lyhkhk@163.com

* Correspondence: yuanyuan.zhang@hainanu.edu.cn

† These authors contributed equally to this work.

Abstract: Salinity is an important environmental factor influencing crop growth and yield. Malate dehydrogenase (MDH) catalyses the reversible conversion of oxaloacetate (OAA) to malate. While many MDHs have been identified in various plants, the biochemical function of MDH in rice remains uncharacterised, and its role in growth and salt stress response is largely unexplored. In this study, the biochemical function of *OsMDH12* was determined, revealing its involvement in regulating tiller number and salt tolerance in rice. *OsMDH12* localises in the peroxisome and is expressed across various organs. In vitro analysis confirmed that *OsMDH12* converts OAA to malate. Seedlings of *OsMDH12*-overexpressing (*OE*) plants had shorter shoot lengths and lower fresh weights than wild-type (*WT*) plants, while *osmdh12* mutants displayed the opposite. At maturity, *OsMDH12-OE* plants had fewer tillers than *WT*, whereas *osmdh12* mutants had more, suggesting *OsMDH12*'s role in tiller number regulation. Moreover, *OsMDH12-OE* plants were sensitive to salt stress, but *osmdh12* mutants showed enhanced salt tolerance. The Na^+/K^+ content ratio increased in *OsMDH12-OE* plants and decreased in *osmdh12* mutants, suggesting that *OsMDH12* might negatively affect salt tolerance through influencing the Na^+/K^+ balance. These findings hint at *OsMDH12*'s potential as a genetic tool to enhance rice growth and salt tolerance.

Keywords: rice; malate dehydrogenase; tiller number; salt tolerance



Citation: Shi, Y.; Feng, J.; Wang, L.; Liu, Y.; He, D.; Sun, Y.; Luo, Y.; Jin, C.; Zhang, Y. *OsMDH12: A Peroxisomal Malate Dehydrogenase Regulating Tiller Number and Salt Tolerance in Rice*. *Plants* **2023**, *12*, 3558.

<https://doi.org/10.3390/plants12203558>

Academic Editors: Joong Hyoun Chin and Hyun-Seung Park

Received: 13 September 2023

Revised: 4 October 2023

Accepted: 8 October 2023

Published: 13 October 2023



Copyright: © 2023 by the authors. Licensee MDPI, Basel, Switzerland. This article is an open access article distributed under the terms and conditions of the Creative Commons Attribution (CC BY) license (<https://creativecommons.org/licenses/by/4.0/>).

1. Introduction

Rice (*Oryza sativa*) is one of the most important food crops worldwide, with over half the global population relying on it as a staple. Tillering is a key agronomic trait that influences grain yield and is affected by both genetic and physiological factors. Therefore, identifying key genes for tiller development is crucial for breeding high-yield crops.

Tiller formation in rice consists of two processes, the initiation of axillary buds on each leaf axil and their further outgrowth [1–3]. During the vegetative growth period, axillary buds persist in forming tillers and spikelets to enhance grain yield [4,5]. However, later axillary buds usually go dormant under the regulation of various hormones [5], which is one of the mechanisms through which rice prevents excessive tillering [6]. Previous studies have shown that auxin and cytokinin play a crucial role in regulating the growth of axillary buds in plants [7,8]. Recently, strigolactones (SLs) have been identified as a unique class of terpenoid lactone phytohormones that control a variety of aspects of plant growth and development, including inhibiting the outgrowth of axillary buds [9]. Over the past decade, many genes involved in SL biosynthesis or the SL signalling pathways have been identified, including *DWARF3 (D3)* [10], *D10* [11], *D14* [12], *D17* [13], *D27* [14],

D53 [15], HIGH TILLERING DWARF1 (HTD1) [16], MORE AXILLARY GROWTH (OsMAX1a, OsMAX1b, OsMAX1c, OsMAX2d and OsMAX1e) [17], OsMADS57 [18], TEOSINTE BRANCHED 1 (OsTB1) [19], IDEAL PLANT ARCHITECTURE 1 (IPA1) [20], OsSH1 [7], and CIRCADIAN CLOCK ASSOCIATED1 (OsCCA1) [21]. In addition, numerous genes involved in other hormone biosynthesis or the signalling pathway have been identified that control the number of rice tillers [3], including LAX PANICLE1 (LAX1) [22], LAX2 [23], MONOCULM1 (MOC1) [24], MOC3 [25], NITROGEN-MEDIATED TILLER GROWTH RESPONSE 5 (NGR5) [26], Hd3a [27], OsDRM2 [28], Cytokinin oxidase/dehydrogenase 2 (CKX2) [29], OsGA2s [30] OsWRKY94 [19], TIF1 [2], and Tiller Number 1 (TN1) [31]. Currently, cloned genes controlling tiller development in rice mainly regulate the initiation or growth of axillary buds. The discovery of these pivotal genes offers important genetic resources and strategies for improving rice yield traits.

Salinity is an important global environmental factor that limits plant growth and crop productivity. To respond to salt stress, plants have evolved several mechanisms to combine endogenous developmental cues with exogenous salinity stress signals to balance growth and stress responses optimally. Ion toxicity and osmotic stress are major factors in the inhibition of plant growth caused by salt stress [32]. To mitigate the damage caused by osmotic stress under salt stress, plants promote the accumulation of protective metabolites in the cytoplasm [33]. These metabolites can function as compatible osmolytes that do not interfere with plant metabolism, including abscisic acid, flavonoids, proline, sugar, glycine betaine, polyamines, and α -amino nitrogen [34,35]. Under salt stress, these osmolytes play a crucial role in osmoregulation by decreasing cellular osmotic potential and stabilizing proteins and cellular structures [35,36]. The metabolomic profile of various plants (*Arabidopsis*, rice, and lotus) shows that the balance between amino acids and organic acids is a conserved response under salt stress [34,37]. Malate is one of the organic acids that affects plant growth, fruit acidity, and nutrient quality and plays an important role in response to salt stress [38–41]. Malate is primarily produced in the cytosol and transported to the vacuole for storage as malic acid [42], an intermediate metabolite of the citric and glyoxylate cycles [43]. Many studies have shown that salt stress leads to the accumulation of malic acid in various plants, including *Arabidopsis* [43], Pear [44], apple [45], grape [46,47], rice [48], and tomato [49]. When plants are exposed to salinity stress, malic acid accumulates and is transported into mitochondria, where it feeds into the tricarboxylic acid cycle to promote mitochondrial ATP production and maintain respiratory flux [38,44,50]. Malate dehydrogenase (MDH) is a class of oxidoreductase enzymes that utilise NAD or NADP(H) as cofactors to catalyse the reversible reaction between malic acid and OAA [51]. This reaction is vital for cellular metabolic processes such as the tricarboxylic acid cycle and the malate–aspartate shuttle in both plants and mammals [52]. Various MDHs have been identified in numerous plant species, including *Arabidopsis thaliana* [43], apple [53], Chinese Fir (*Cunninghamia lanceolata*) [54], cotton [55], maize [56], melon [57], poplar (*Populus trichocarpa*) [58], tobacco [59], tomato [60], soybean [61], *Stylosanthes* (*Stylosanthes guianensis*) [62], and rice [48]. Some have been found to be essential for several anabolic and catabolic processes, converting OAA to malic acid. For instance, *ZmMDH4* [63], *GhmMDH1* [64], and *MdcyMDH1* [40] are known to catalyse the conversion of OAA to malate in maize, cotton, and apples. While the biochemical function of MDH is established, its biological function in plants is not yet fully understood.

In rice, twelve MDH (*OsMDH1*–*OsMDH12*) members are present. *OsMDH1* is a plastid-localised protein that negatively regulates salt tolerance through affecting vitamin B6 content [65]. *OsMDH10/FLO16* encodes a NAD-dependent cytosolic malate dehydrogenase. Knockout of *OsMDH10/FLO16* notably reduces the starch content in grains, whereas its overexpression significantly increases grain weight, suggesting that *OsMDH10* is vital for starch biosynthesis and seed development [66]. Recent studies indicate that natural variations in the promoter region of *OsMDH8* may be linked to salt tolerance during the rice seedling stage [48]. Most MDH family genes are significantly induced by salt stress [48], implying a potential role in rice's salt stress response. However, the role

of the majority of *OsMDH* genes in plant development and in responding to salt stress remains largely unexplored.

In this study, we functionally characterised *OsMDH12*, which is localised in the peroxisome. We found that *OsMDH12* serves as a negative regulator of both tiller number and salt tolerance in rice.

2. Results

2.1. Phylogenetic Tree, Expression Profiles, and Subcellular Localization of *OsMDH12*

The full-length 1071 bp cDNA sequence of *OsMDH12* (Os12g0632700) encodes a malate dehydrogenase that is predicted to be 357 amino acids long, according to the Rice Genome Annotation Project (<http://rice.plantbiology.msu.edu> (accessed on 1 May 2021)).

A phylogenetic tree was constructed using the amino acid sequences of *OsMDH12* and malate dehydrogenases from other plants, such as *Arabidopsis*, maize, and tomato. *OsMDH12* displays high amino acid sequence similarity to *AtpMDH1*, *AtpMDH2*, *ZmMDH12*, *ZmMDH13*, *SIMDH2*, *SIMDH3*, and *OsMDH3* (Figure 1A).

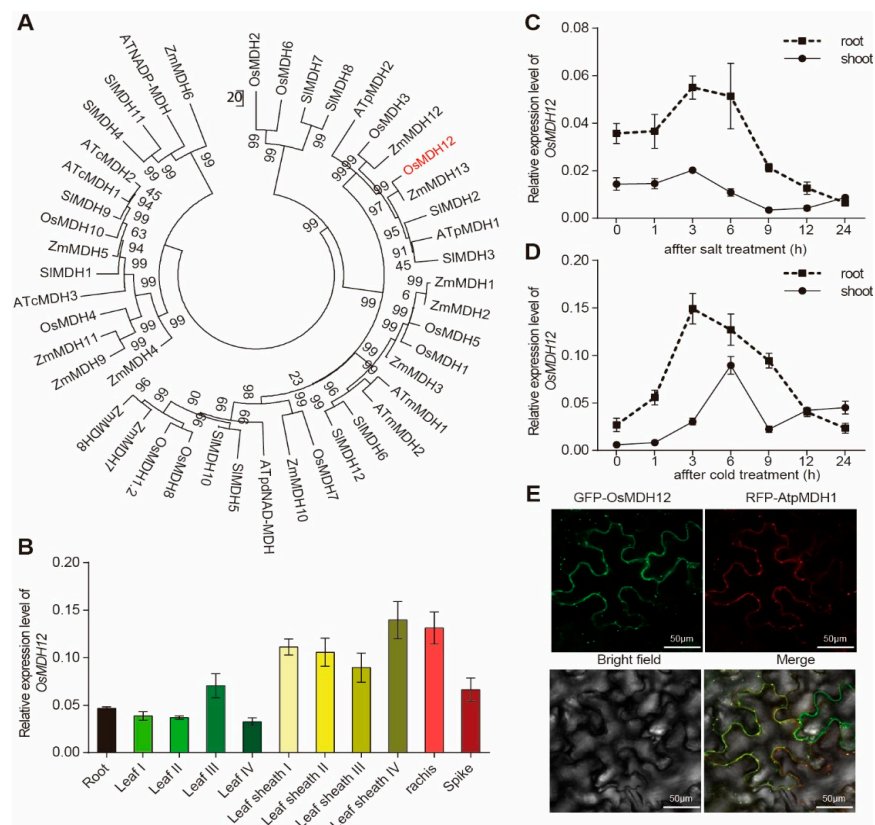


Figure 1. Expression pattern of *OsMDH12*. (A) Phylogenetic relationship of MDH proteins in rice, *Arabidopsis*, and tomato. Bootstrap values from 1000 trials are indicated. (B) Expression levels of *OsMDH12* in different rice organs. Samples were taken from Zhonghua11 grown in a paddy field. (C,D) Time-course expression of *OsMDH12* under salt (C) and cold (D) treatment. Standard deviations are based on three biological replicates. (E) Subcellular localization of *OsMDH12* protein in leaves of *N. benthamiana*. 35S:GFP-*OsMDH12* and 35S:RFP:*AtpMDH1* were co-transformed into the leaves of *Nicotiana benthamiana*. *AtpMDH1* serves as a peroxisome marker. The scale is set at 50 μ m.

To assess the function of *OsMDH12*, we first analysed its expression pattern in various organs. Quantitative real-time PCR (qRT-PCR) revealed that *OsMDH12* is expressed in all tissues examined, including roots, stems, leaves, and spikes (Figure 1B). Subsequently, we explored the expression of *OsMDH12* under abiotic stress conditions. The transcription

level of OsMDH12 in rice leaves and roots was detected after salt and cold treatment. The results indicated that the transcript level of *OsMDH12* was strongly induced by both salt and cold stress (Figure 1C,D).

To ascertain the subcellular localization of OsMDH12, the coding sequence of the full-length *OsMDH12* was fused to Green Fluorescent Protein (GFP) under the control of the CaMV35S promoter. Colocalization with the peroxisome protein AtpMDH1 [67] in the leaf epidermal cells of *Nicotiana benthamiana* confirmed a peroxisomal location for OsMDH12 (Figure 1E).

2.2. Enzyme Analysis of *OsMDH12*

Malate dehydrogenase (MDH) has been shown to catalyse the reversible reaction between malic acid and OAA, using NAD or NADP(H) as cofactors (Figure 2A). To ascertain the biochemical function of OsMDH12, we conducted enzymatic assays *in vitro* using recombinant OsMDH12 proteins. Our results demonstrated that OsMDH12 displayed high activity when OAA was used as the donor (Figure 2B). Conversely, no activity was detected when malate served as the donor (Figure 2B), suggesting that OsMDH12 catalyses the conversion of OAA to malate.

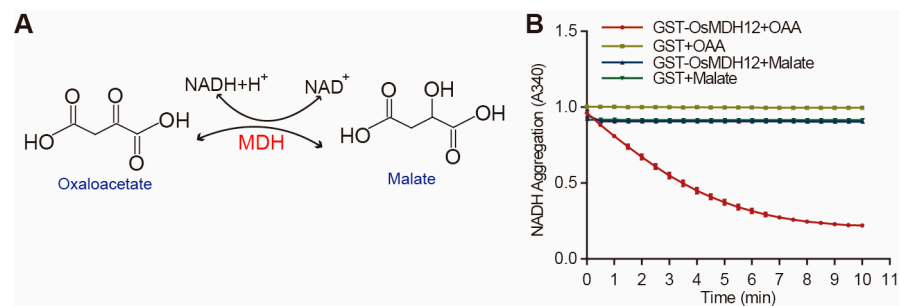


Figure 2. OsMDH12 catalyses OAA to malate. (A) Schematic diagram of the enzyme-catalysed reaction by Bend OsMDH12. (B) Assays of OsMDH12 activity. The assay was conducted in the presence of GST-OsMDH12, GST, NADH, and OAA. Data are expressed as the decrease in OD at 340 nm over time.

2.3. Molecular Characterization of MDH12-OE and *osmdh12* Knockout Mutant Plants

To investigate the function of *OsMDH12* in rice, we generated *OsMDH12*-overexpressing (*OsMDH12*-OE1 and *OsMDH12*-OE2) (Figure 3A) and *osmdh12* CRISPR (*osmdh12*-1 and *osmdh12*-2) lines (Figure 3B) in the japonica cultivar Zhonghua11 (ZH11) background. *osmdh12*-1 carried a one-base insertion (T) in the target site, and *osmdh12*-2 carried a two-base deletion (TC) in the target site, which all truncated the *OsMDH12* open reading frame (Figure 3A). At the seedling stage, growth in the *OsMDH12*-OE plants was inhibited, showing significantly decreased shoot lengths and fresh weights (Figure 3C–E). In contrast, the *osmdh12* mutants displayed a significant increase in shoot lengths and fresh weights (Figure 3C–E). Additionally, malate content was reduced in the *osmdh12* mutant lines compared to the WT (Figure 3F). These results suggested that *MDH12* negatively regulates growth but positively regulates malic acid content in rice.

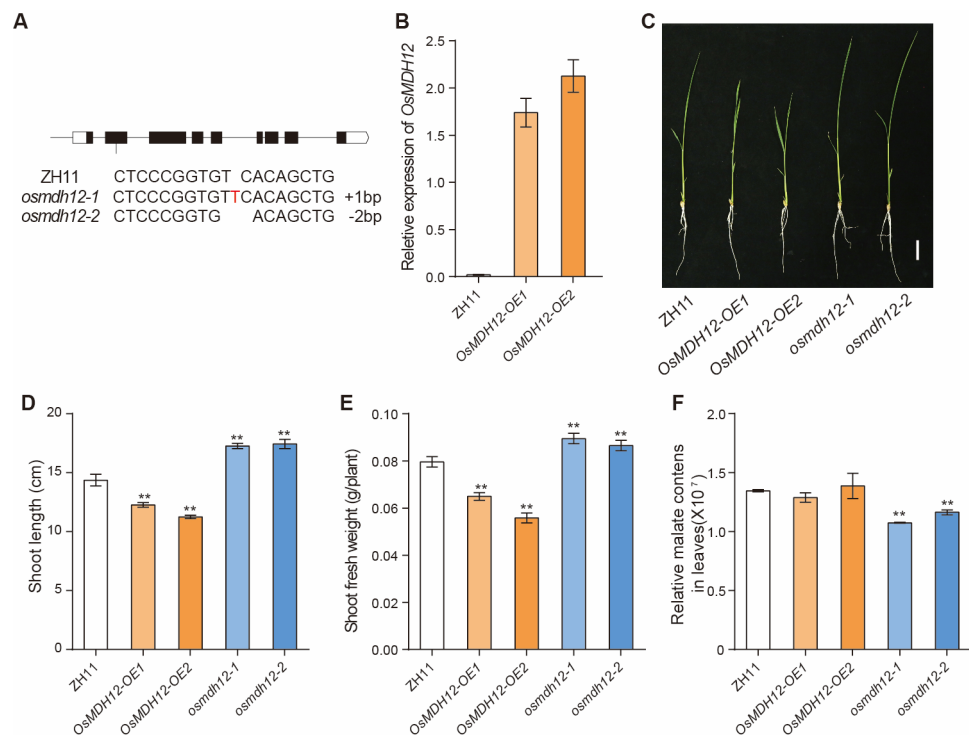


Figure 3. Appearance and malate contents of *OsMDH12* transgenic lines at the seedling stage. (A) The *osmdh12* knockout mutants were generated using CRISPR gene editing technology. (B) Expression level of *OsMDH12* in two independent overexpressing lines. (C) Phenotype comparison of ZH11, *OsMDH12-OE* lines, and *osmdh12* mutants (two different CRISPR lines) at the seedling stage. The scale is set at 2 cm. (D,E) Plant height (D) and fresh weight (E) in ZH11, *OsMDH12-OE*, and *osmdh12* mutants. (F) Malate content in ZH11, *OsMDH12-OE*, and *osmdh12* mutants. Values are presented as mean \pm SD (n = 10); ** $p < 0.01$ (*t*-test).

2.4. MDH12 Negatively Regulates Tiller Numbers in Rice

To further explore the physiological functions of *OsMDH12*, we observed the phenotypes of *OsMDH12-OE* and *osmdh12* mutant plants at the mature stage. When grown in a paddy field, no significant difference in plant height was observed between the *osmdh12* mutant and the WT (Figure 4A,B). However, *OsMDH12-OE* plants displayed fewer tillers compared to WT plants (Figure 4C). Conversely, *osmdh12* plants had a greater number of tillers, indicating that *OsMDH12* negatively regulates tiller numbers in rice (Figure 4C). We then searched a publicly available genetic co-expression database (CREP, <http://crep.ncpgr.cn/> (accessed on 1 June 2022)) to identify genes co-expressed with *OsMDH12* that are involved in regulating tiller number in rice. *OsMDH12* exhibited a high correlation coefficient with three genes (*PAY1*, *TN1*, and *OsTOM2*) implicated in tiller number [31,68,69] (Figure 4D, Table S2). To investigate whether the expression levels of *PAY1*, *TN1*, and *OsTOM2* were affected in *osmdh12* mutant plants, we performed qRT-PCR analysis. The results revealed that the expression of *PAY1* and *TN1* in the shoots was not significantly different between *OsMDH12-OE* and *osmdh12* mutant plants compared to WT (Figure 4E,F). However, the expression of *OsTOM2* was repressed in the shoots of *OsMDH12-OE* plants but was upregulated in the roots of the *osmdh12* mutant (Figure 4G). These findings suggest that *OsMDH12* regulates tiller number through affecting the expression of *OsTOM2* in rice.

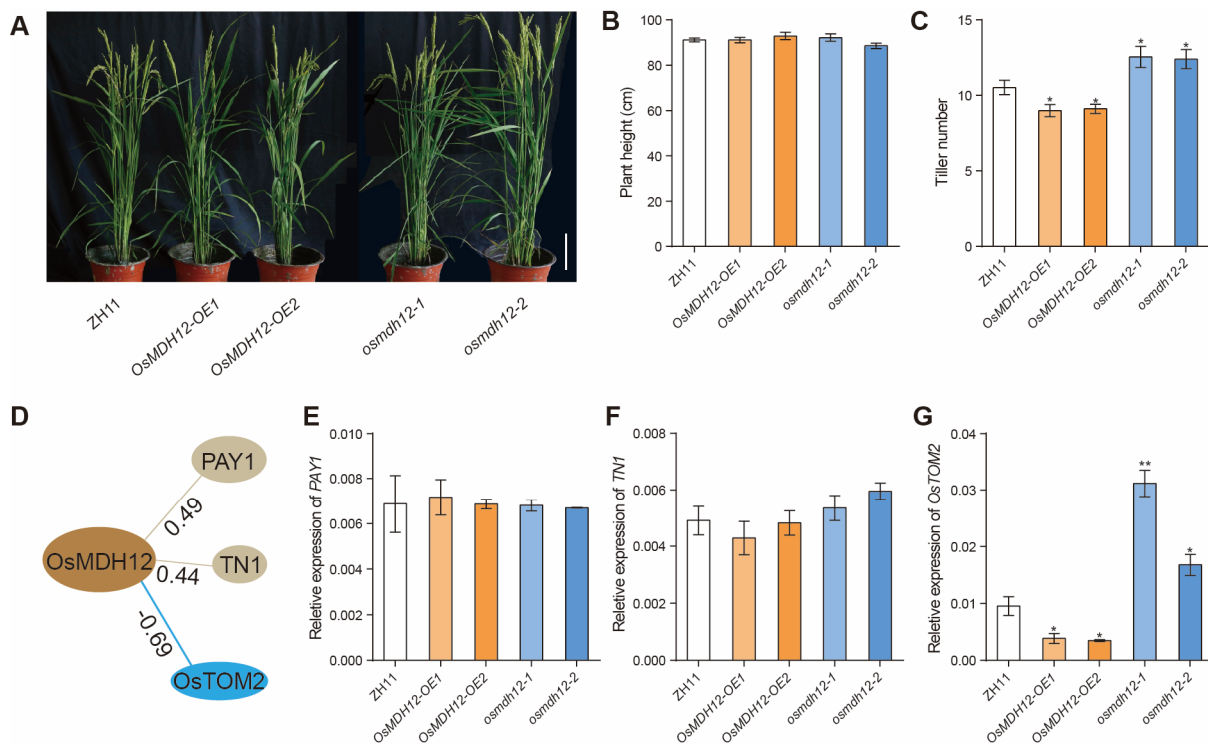


Figure 4. *OsMDH12* regulates tiller numbers in rice. **(A)** Phenotypic comparison between WT and *OsMDH12* transgenic plants at the maturity stage. The scale is set at 10 cm. **(B,C)** Plant height and tiller number in ZH11, *OsMDH12-OE*, and *osmdh12* mutant. **(D)** Genes co-expressed with *OsMDH12* related to tillering. **(E–G)** Expression levels of *PAY1* (**E**), *TN1* (**F**), and *OsTOM2* (**G**) in ZH11, *OsMDH12-OE*, and *osmdh12* mutant. Values are presented as the mean \pm SD ($n = 10$); * $p < 0.05$, ** $p < 0.01$ (t -test).

2.5. *OsMDH12* Negatively Regulates Salt Tolerance in Rice

To explore the role of *OsMDH12* in salt tolerance, we induced salinity stress in *OsMDH12-OE* and *osmdh12* mutant plants. Under normal growth conditions, no noticeable phenotypic differences were observed between *OsMDH12* transgenic and WT plants (Figure 5A). However, when subjected to 150 mM NaCl treatment (Figure 5B,C), *OsMDH12-OE* plants exhibited salt-sensitive phenotypes, characterised by lower survival rates (Figure 5D) and increased ROS accumulation (Figure 5E). Conversely, *osmdh12* mutants displayed enhanced salt stress tolerance. We then analysed the Na^+/K^+ content ratio in both *OsMDH12* transgenic and WT plants. The results revealed that the Na^+/K^+ content ratio significantly increased in *OsMDH12-OE* plants but decreased in *osmdh12* mutant plants (Figure 5F). These findings suggest that *OsMDH12* negatively regulates salt tolerance through affecting the Na^+/K^+ ratio in rice.

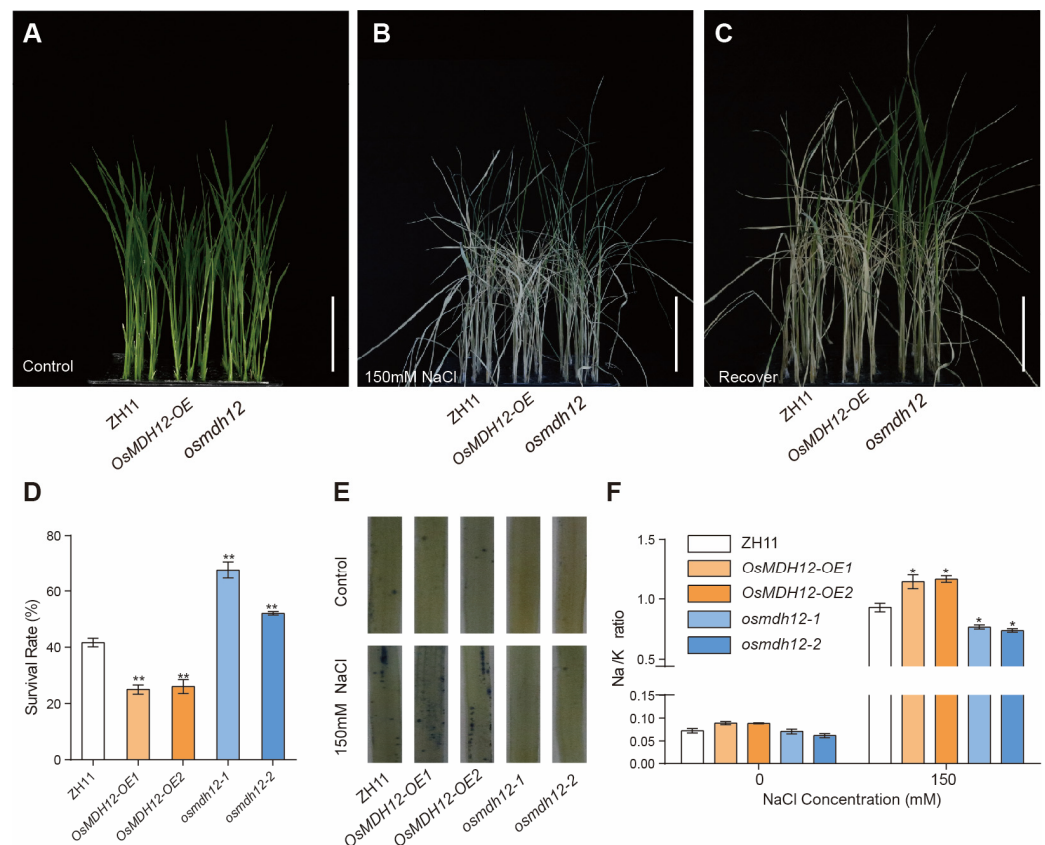


Figure 5. Performance of *OsMDH12* transgenic plants under salt stress. (A–C) Two-week-old rice seedlings from ZH11, *OsMDH12-OE*, and *osmdh12* plants (A) were treated with 150 mM NaCl for seven days (B) and then allowed to recover for three days (C). The scale is set at 5 cm. (D) Survival rate under salt stress. (E) Phenotype revealed by NBT staining after 24 h of salt stress. (F) Na⁺/K⁺ ratio in ZH11, *OsMDH12-OE*, and *osmdh12* mutants. Values represent the mean \pm SD (n = 3); * $p < 0.05$, ** $p < 0.01$ (*t*-test).

3. Discussion

In this study, we characterised the function of *OsMDH12*, a member of the rice MDH gene family, and identified its negative regulatory role in controlling tiller number and salt tolerance. Malate dehydrogenase catalyses the reversible conversion of malate and oxaloacetate (OAA) using NADH or NADPH as coenzymes. NADP-dependent MDH isoforms are primarily localised in chloroplasts, while NAD-dependent MDH isoforms are found in other organelles, including the cytoplasm, mitochondria, glycosomes, peroxisomes, and chloroplasts [43]. Our data demonstrate that *OsMDH12* is an NADP-dependent MDH isoform which is localised to the peroxisome and catalyses the conversion of OAA to malate in rice (Figures 1 and 2).

Members of the MDH family are crucial for root growth [57], seed germination [66] and maturation [70], and embryo development [43]. In *Arabidopsis*, the suppression of NAD⁺-dependent plastidial MDH (*pdnad-mdh*) leads to embryonic lethality, while reduced expression of *pdnad-mdh* results in dwarfism, diminished chlorophyll levels, lowered photosynthetic rates, reduced daytime carbohydrate levels, and chloroplast disorganization [51,68]. In rice, *OsMDH10* has been implicated in starch biosynthesis and seed development [40]. *OsMDH12* shares high homology with *Arabidopsis* AtpMDH1 and AtpMDH2, suggesting functional similarities (Figure 1). In *Arabidopsis*, the *mmdh1/mmdh2* double mutants exhibit significantly reduced growth and photosynthesis rates compared to the WT [69,70]. Similar phenotypes were observed in *osmdh12* mutants during the seedling stage, including decreased plant height and fresh weight (Figure 3). These findings suggest that the functions of MDH genes are conserved in both rice and *Arabidopsis*. However, unlike previous

studies on *MDH* genes in plants [43,57,66,71], we found that *OsMDH12* plays a pivotal role in regulating rice tiller number.

Tiller number, a crucial yield component, is a target for genetic improvement in crops [72]. Elements, both macronutrients and micronutrients, significantly influence plant growth and the degree of tillering in rice [68,73]. For example, iron (Fe) limitation hampers rice growth, reduces height, and restricts tiller numbers. *OsTOM2*, part of the major facilitator superfamily (MFS), is a 2'-deoxymugineic acid (DMA) transporter that mediates DMA secretion from roots to the rhizosphere and is involved in Fe mobilization via DMA secretion into the vascular bundles for phloem/xylem metal loading [74]. Inhibition of *OsTOM2* expression markedly reduces tiller number, dry weight, and yield in rice, implying that *OsTOM2* is essential for optimal growth [68]. We observed similar phenotypes in *OsMDH12*-overexpressing plants, which displayed fewer tillers and reduced dry weights (Figure 4). Moreover, the expression of *OsTOM2* was significantly decreased in *OsMDH12*-overexpressing plants, while it increased in *OsMDH12* mutant plants, suggesting that *OsMDH12* may regulate tiller number via *OsTOM2* expression. The role of *OsMDH12* in metal mobilization warrants further investigation.

Several studies have demonstrated that MDH genes play significant roles in plant responses to various abiotic stresses [40,54,57], particularly in salt stress resistance [48,65]. For instance, the overexpression of plastid maize NADP-malate dehydrogenase (*ZmNADP-MDH*) in *Arabidopsis* enhances its salt stress tolerance [70]. In apples, overexpressing cytosolic NAD-malate dehydrogenase (*MdcyMDH*) results in increased salt tolerance and decreased ROS levels [63]. Recent research has shown that *OsMDH1*, a plastid NAD-dependent dehydrogenase, negatively regulates salt stress in rice [64]. Further analysis indicated that *OsMDH1* modulates the response to salt stress through affecting vitamin B6 levels [64]. Despite the differing subcellular localizations of *OsMDH1* and *OsMDH12*, the phenotypes of transgenic plants overexpressing either gene were similar (Figure 5). Lines overexpressing *OsMDH1* or *OsMDH12* are sensitive to salt stress, while lines with a knockout of *OsMDH1* or *OsMDH12* show tolerance to salt stress. In contrast to *OsMDH1*, our findings suggest that *OsMDH12*-mediated salt tolerance is closely linked to an imbalance in the K^+/Na^+ ratio. Whether *OsMDH12* is involved in the regulation of vitamin B6 synthesis remains an open question for further study.

In conclusion, we have uncovered the biological function of *OsMDH12*, a member of the malate dehydrogenase family. Our results show that *OsMDH12* encodes a peroxisomal malate dehydrogenase that converts OAA to malate. Moreover, we demonstrate that *OsMDH12* plays an essential role in regulating both plant growth and the response to salt stress.

4. Materials and Methods

4.1. Phylogenetic Analysis

The *OsMDH* protein sequences were extracted from the TIGR database (<http://rice.uga.edu/> (accessed on 1 May 2021)). The MDH protein sequences of *Arabidopsis* (*AtMDH*), tomato (*SIMDH*), and maize (*ZmMDH*) were obtained from the National Center for Biotechnology Information (NCBI, Bethesda, MD, USA, <https://www.ncbi.nlm.nih.gov/> (accessed on 1 May 2021)). These sequences were aligned using MEGA 6 (Temple University, Philadelphia, PA, USA) software, and a neighbour-joining (NJ) tree was generated with 1000 bootstrap replicates; all other parameters were set to their default values.

4.2. Plant Materials and Stress Treatments

All plant materials used in this study were either ZH11 or derived from this cultivar. The *osmdh12* mutants were generated using the CRISPR-Cas9 system, while *OsMDH12-OE* plants were produced under the control of the maize ubiquitin promoter in ZH11. The full-length coding sequence of *OsMDH12* was amplified from Nipponbare (NIP) cultivar and cloned into the pJC034 vector. For physiological analyses, seedlings were cultivated in paddy fields in Lingshui, Hainan Province, China. For salt treatments, seeds were

germinated for 3 days at 37 °C and then incubated in culture solution at 28 °C for 7 days. Following this, the seedlings were transferred to a 150 mmol/L NaCl solution for an additional 7 days. Seeds were then allowed to recover in a nutrient solution for 7 days [75]. Shoot and root growth seedlings were estimated as surviving seedlings. Thirty plants of ZH11 and *OsMDH12* transgenic lines for each experiment were used for subsequent statistical calculations. For cold treatment, the seedlings were exposed to 6 °C [76]. Leaves were sampled at 1 h, 3 h, 6 h, 9 h, 12 h, and 24 h intervals.

4.3. Gene Transcription Analysis

qRT-PCR was conducted to assess gene expression following salt or cold treatments. Leaves from various treatment groups were harvested at different time points post-treatment. All samples were processed using the RNA isolator Total RNA Extraction Reagent (Vazyme, Nanjing, China), and first-strand cDNA was synthesised using EasyScript One-step gDNA Removal and cDNA Synthesis SuperMix (TRANSGEN, Beijing, China), as per the manufacturer's instructions. Primers for gene specificity were designed using Primer 5.0 and are listed in Supplemental Table S1. The internal reference used was the Ubiquitin5 gene. qRT-PCR was carried out on an ABI 7500 Real-Time PCR system (Applied Biosystems, Waltham, MA, USA), utilizing a SYBR Premix Ex Taq Kit in accordance with the manufacturer's guidelines. All reactions were conducted in a minimum of three biological replicates.

4.4. Subcellular Localization

The full-length coding sequence of *OsMDH12* was cloned into the pH7GWFS2.0 vector to generate 35S:EGFP-*OsMDH12*. Similarly, AtpMDH1, a peroxisome marker, was cloned into the same vector to produce 35S:RFP-AtpMDH1 [60]. Both 35S:EGFP-*OsMDH12* and 35S:RFP-AtpMDH1 were transiently expressed in *N. benthamiana* leaves with agrobacterium EHA105 and imaged using a laser confocal microscope (LSM980; Zeiss, Jena, Germany) after 2 days of incubation at 22 °C.

4.5. OsMDH Activity Assays

The full-length coding sequence of *OsMDH12* was cloned into the pDEST15 vector using the Gateway recombination reaction (Invitrogen, Waltham, MA, USA). Expression constructs were introduced into BL21 (DE3) cells, and the expression of the fusion proteins was induced with 0.1 mM IPTG when the bacterial culture reached an OD₆₀₀ of 0.5. After incubation at 16 °C for 14 h, cells were harvested via centrifugation and resuspended in 50 mL of Lysis Buffer containing Tris-HCl (50 mM), NaCl (50 mM), 5% glycerol, and PMSF (0.1 mM). Cells were disrupted using a pressure crusher, and the soluble protein fractions were subsequently centrifuged [77]. Purification was carried out and monitored using a GST resin filter column for GST-tagged proteins. *OsMDH12* activity was assessed through the spectrophotometric measurement of NADH consumption at 340 nm. The reaction was conducted in a 250 mM HEPES (pH 8.0) buffer containing MgCl₂ (2 mM), NAD⁺/NADH (0.25 mM), and either OAA or malate (2.5 mM). Purified *OsMDH12*-GST or GST (5 µg) was added to a 200 µL reaction volume. All reactions were conducted in a minimum of three replicates.

4.6. Measurement of Malate

The liquid chromatography–tandem mass spectrometry (LC-MS/MS) system (QTRAP 6500, AB SCIEX, Toronto, ON, Canada) was used to determine the content of malate as previously described [73]. All samples were rushed using a high-throughput tissue grinder (MM400, Retsch, Haan, Germany) after freeze-drying. The dry powder was extracted with 70% aqueous methanol containing lidocaine as the internal standard (0.1 mg/L) overnight at 4 °C. Following centrifugation at 1000× g for 5 min, the lipids were absorbed and filtered using a 0.22 µm pore size nylon syringe filter (SCAA-104, ANPEL, Shanghai, China) before the LC-MS analysis. For LC-MS analysis, a C18 column (Shim-pack GISS, SHIMADZU, Kyoto, Japan, 2.1 mm × 100 mm, 1.9 µm) was equipped. A 2 µL sample

was eluted by mobile phase at 0.3 mL/min flow rate at 40 °C. Three biological replicates were measured for each transgenic line.

4.7. NBT Staining

For the NBT assay, small pieces of the second leaf from 14-day-old seedlings were vacuum-filtered in 0.1% (*w/v*) NBT for 30 min and then incubated for 10 h under ambient conditions. After draining the solution, 95% ethanol was added to decolourise the sample at 80 °C until the solution became colourless.

4.8. Determination of Sodium and Potassium Concentrations

The rice was harvested seven days after the initiation of salt treatment and was rinsed three times with distilled water. Samples were digested in nitric acid in a microwave (Multivave Pro 41, Anton Paaranton Paar, Graz, Austria) for 1 h, as previously described [78]. Sodium and potassium ion concentrations were measured using ICP-MS (ICP-MS 7800, Agilent, Santa Clara, CA, USA) after dilution in deionised water. Three biological replicates were measured for each transgenic line.

4.9. Statistical Analysis

Plant phenotype, the content of malate, gene expression, survival rate, and Na⁺/K⁺ ratio were analysed via one-way or two-way ANOVA using Microsoft Excel software (Office_Professional_Plus_2016) and corrected with Student's *t*-test at a significance level of 0.05.

4.10. Accession Numbers

The accession numbers of genes in this article are as follows: OsMDH12 (Os12g0632700), PAY1 (Os08g0407200), TN1 (Os01g0610300), and OsTOM2 (Os11g0135000). Sequence data from this article can be found in the Rice Genome Annotation Project website (<http://rice.plantbiology.msu.edu/> (accessed on 1 May 2021)) and NCBI (<https://www.ncbi.nlm.nih.gov/> (accessed on 1 May 2021)).

Supplementary Materials: The following supporting information can be downloaded at <https://www.mdpi.com/article/10.3390/plants12203558/s1>. Table S1: The primers used in this study; Table S2: The Co-expression analysis of OsMDH12.

Author Contributions: Y.Z. and C.J. designed the experiments; Y.S. (Yuheng Shi), J.F., and L.W. conducted most of the experiments with assistance from Y.L. (Yanchen Liu), D.H., Y.S. (Yangyang Sun), and (Yuehua Luo); C.J. revised the paper; Y.S. (Yuheng Shi) and Y.Z. wrote and finalized the paper. All authors have read and agreed to the published version of the manuscript.

Funding: This research was funded by the Hainan Major Science and Technology Project (No. ZDKJ202001), the Natural Science Foundation of Hainan Province (Nos. 321RC476, 321RC460, and 321MS004), the Technology Innovation Special Project of Sanya (No. 2022KJCX54), and the Hainan Yazhou Bay Seed Laboratory (No. B21Y10902).

Data Availability Statement: All data are available upon reasonable request.

Conflicts of Interest: The authors declare no conflict of interest.

References

1. Stirnberg, P.; van de Sande, K.; Leyser, H.M.O. MAX1 and MAX2 control shoot lateral branching in Arabidopsis. *Development* **2002**, *129*, 1131–1141. [[CrossRef](#)]
2. Shao, G.; Lu, Z.; Xiong, J.; Wang, B.; Jing, Y.; Meng, X.; Liu, G.; Ma, H.; Liang, Y.; Chen, F.; et al. Tiller Bud Formation Regulators MOC1 and MOC3 Cooperatively Promote Tiller Bud Outgrowth by Activating FON1 Expression in Rice. *Mol. Plant* **2019**, *12*, 1090–1102. [[CrossRef](#)] [[PubMed](#)]
3. Yan, Y.; Ding, C.; Zhang, G.; Hu, J.; Zhu, L.; Zeng, D.; Qian, Q.; Ren, D. Genetic and environmental control of rice tillering. *Crop. J.* **2023**. [[CrossRef](#)]
4. Li, Y.; He, Y.; Liu, Z.; Qin, T.; Wang, L.; Chen, Z.; Zhang, B.; Zhang, H.; Li, H.; Liu, L.; et al. OsSPL14 acts upstream of OsPIN1b and PILS6b to modulate axillary bud outgrowth by fine-tuning auxin transport in rice. *Plant J.* **2022**, *111*, 1167–1182. [[CrossRef](#)]

5. Wang, Y.; Li, J. Branching in rice. *Curr. Opin. Plant Biol.* **2011**, *14*, 94–99. [[CrossRef](#)] [[PubMed](#)]
6. Kotov, A.A.; Kotova, L.M.; Romanov, G.A. Signaling network regulating plant branching: Recent advances and new challenges. *Plant Sci.* **2021**, *307*, 110880. [[CrossRef](#)] [[PubMed](#)]
7. Duan, E.; Wang, Y.; Li, X.; Lin, Q.; Zhang, T.; Wang, Y.; Zhou, C.; Zhang, H.; Jiang, L.; Wang, J.; et al. OsSHI1 Regulates Plant Architecture through Modulating the Transcriptional Activity of IPA1 in Rice. *Plant Cell* **2019**, *31*, 1026–1042. [[CrossRef](#)] [[PubMed](#)]
8. Zürcher, E.; Müller, B. Cytokinin Synthesis, Signaling, and Function—Advances and New Insights. *Int. Rev. Cell Mol. Biol.* **2016**, *324*, 1–38. [[CrossRef](#)]
9. Umehara, M.; Hanada, A.; Yoshida, S.; Akiyama, K.; Arite, T.; Takeda-Kamiya, N.; Magome, H.; Kamiya, Y.; Shirasu, K.; Yoneyama, K.; et al. Inhibition of shoot branching by new terpenoid plant hormones. *Nature* **2008**, *455*, 195–200. [[CrossRef](#)] [[PubMed](#)]
10. Zhao, J.; Wang, T.; Wang, M.; Liu, Y.; Yuan, S.; Gao, Y.; Yin, L.; Sun, W.; Peng, L.; Zhang, W.; et al. DWARF3 Participates in an SCF Complex and Associates with DWARF14 to Suppress Rice Shoot Branching. *Plant Cell Physiol.* **2014**, *55*, 1096–1109. [[CrossRef](#)]
11. Zhang, S.; Li, G.; Fang, J.; Chen, W.; Jiang, H.; Zou, J.; Liu, X.; Zhao, X.; Li, X.; Chu, C.; et al. The Interactions among DWARF10, Auxin and Cytokinin Underlie Lateral Bud Outgrowth in Rice. *J. Integr. Plant Biol.* **2010**, *52*, 626–638. [[CrossRef](#)]
12. Arite, T.; Umehara, M.; Ishikawa, S.; Hanada, A.; Maekawa, M.; Yamaguchi, S.; Kyoizuka, J. d14, a Strigolactone-Insensitive Mutant of Rice, Shows an Accelerated Outgrowth of Tillers. *Plant Cell Physiol.* **2009**, *50*, 1416–1424. [[CrossRef](#)]
13. Wang, Y.; Shang, L.; Yu, H.; Zeng, L.; Hu, J.; Ni, S.; Rao, Y.; Li, S.; Chu, J.; Meng, X.; et al. A Strigolactone Biosynthesis Gene Contributed to the Green Revolution in Rice. *Mol. Plant* **2020**, *13*, 923–932. [[CrossRef](#)]
14. Lin, H.; Wang, R.; Qian, Q.; Yan, M.; Meng, X.; Fu, Z.; Yan, C.; Jiang, B.; Su, Z.; Li, J.; et al. DWARF27, an Iron-Containing Protein Required for the Biosynthesis of Strigolactones, Regulates Rice Tiller Bud Outgrowth. *Plant Cell* **2009**, *21*, 1512–1525. [[CrossRef](#)] [[PubMed](#)]
15. Zhou, F.; Lin, Q.; Zhu, L.; Ren, Y.; Zhou, K.; Shabek, N.; Wu, F.; Mao, H.; Dong, W.; Gan, L.; et al. D14–SCFD3-dependent degradation of D53 regulates strigolactone signalling. *Nature* **2013**, *504*, 406–410. [[CrossRef](#)]
16. Zou, J.; Zhang, S.; Zhang, W.; Li, G.; Chen, Z.; Zhai, W.; Zhao, X.; Pan, X.; Xie, Q.; Zhu, L. The rice HIGH-TILLERING DWARF1 encoding an ortholog of Arabidopsis MAX3 is required for negative regulation of the outgrowth of axillary buds. *Plant J.* **2006**, *48*, 687–698. [[CrossRef](#)] [[PubMed](#)]
17. Wang, X.; Liang, Y.; Li, L.; Gong, C.; Wang, H.; Huang, X.; Li, S.; Deng, Q.; Zhu, J.; Zheng, A.; et al. Identification and Cloning of TILLERING-Related Genes OsMAX1 in Rice. *Rice Sci.* **2015**, *22*, 255–263. [[CrossRef](#)]
18. Guo, S.; Xu, Y.; Liu, H.; Mao, Z.; Zhang, C.; Ma, Y.; Zhang, Q.; Meng, Z.; Chong, K. The interaction between OsMADS57 and OsTB1 modulates rice tillering via DWARF14. *Nat. Commun.* **2013**, *4*, 1566. [[CrossRef](#)] [[PubMed](#)]
19. Chen, L.; Zhao, Y.; Xu, S.; Zhang, Z.; Xu, Y.; Zhang, J.; Chong, K. OsMADS57 together with OsTB1 coordinates transcription of its target OsWRKY94 and D14 to switch its organogenesis to defense for cold adaptation in rice. *New Phytol.* **2018**, *218*, 219–231. [[CrossRef](#)]
20. Lu, Z.; Yu, H.; Xiong, G.; Wang, J.; Jiao, Y.; Liu, G.; Jing, Y.; Meng, X.; Hu, X.; Qian, Q.; et al. Genome-Wide Binding Analysis of the Transcription Activator IDEAL PLANT ARCHITECTURE1 Reveals a Complex Network Regulating Rice Plant Architecture. *Plant Cell* **2013**, *25*, 3743–3759. [[CrossRef](#)]
21. Wang, F.; Han, T.; Song, Q.; Ye, W.; Song, X.; Chu, J.; Li, J.; Chen, Z.J. The Rice Circadian Clock Regulates Tiller Growth and Panicle Development through Strigolactone Signaling and Sugar Sensing. *Plant Cell* **2020**, *32*, 3124–3138. [[CrossRef](#)]
22. Oikawa, T.; Kyoizuka, J. Two-Step Regulation of LAX PANICLE1 Protein Accumulation in Axillary Meristem Formation in Rice. *Plant Cell* **2009**, *21*, 1095–1108. [[CrossRef](#)]
23. Tabuchi, H.; Zhang, Y.; Hattori, S.; Omae, M.; Shimizu-Sato, S.; Oikawa, T.; Qian, Q.; Nishimura, M.; Kitano, H.; Xie, H.; et al. LAX PANICLE2 of Rice Encodes a Novel Nuclear Protein and Regulates the Formation of Axillary Meristems. *Plant Cell* **2011**, *23*, 3276–3287. [[CrossRef](#)] [[PubMed](#)]
24. Liao, Z.; Yu, H.; Duan, J.; Yuan, K.; Yu, C.; Meng, X.; Kou, L.; Chen, M.; Jing, Y.; Liu, G.; et al. SLR1 inhibits MOC1 degradation to coordinate tiller number and plant height in rice. *Nat. Commun.* **2019**, *10*, 1–9. [[CrossRef](#)]
25. Lu, Z.; Shao, G.; Xiong, J.; Jiao, Y.; Wang, J.; Liu, G.; Meng, X.; Liang, Y.; Xiong, G.; Wang, Y.; et al. MONOCULM 3, an Ortholog of WUSCHEL in Rice, Is Required for Tiller Bud Formation. *J. Genet. Genom.* **2015**, *42*, 71–78. [[CrossRef](#)] [[PubMed](#)]
26. Wu, K.; Wang, S.; Song, W.; Zhang, J.; Wang, Y.; Liu, Q.; Yu, J.; Ye, Y.; Li, S.; Chen, J.; et al. Enhanced sustainable green revolution yield via nitrogen-responsive chromatin modulation in rice. *Science* **2020**, *367*, 641. [[CrossRef](#)]
27. Tsuji, H.; Tachibana, C.; Tamaki, S.; Taoka, K.-I.; Kyoizuka, J.; Shimamoto, K. Hd3a promotes lateral branching in rice. *Plant J.* **2015**, *82*, 256–266. [[CrossRef](#)]
28. Moritoh, S.; Eun, C.-H.; Ono, A.; Asao, H.; Okano, Y.; Yamaguchi, K.; Shimatani, Z.; Koizumi, A.; Terada, R. Targeted disruption of an orthologue of domains rearranged methylase 2, OsDRM2, impairs the growth of rice plants by abnormal DNA methylation. *Plant J.* **2012**, *71*, 85–98. [[CrossRef](#)] [[PubMed](#)]
29. Yeh, S.-Y.; Chen, H.-W.; Ng, C.-Y.; Lin, C.-Y.; Tseng, T.-H.; Li, W.-H.; Ku, M.S.B. Down-Regulation of Cytokinin Oxidase 2 Expression Increases Tiller Number and Improves Rice Yield. *Rice* **2015**, *8*, 1–13. [[CrossRef](#)]
30. Lo, S.-F.; Yang, S.-Y.; Chen, K.-T.; Hsing, Y.-I.; Zeevaert, J.A.; Chen, L.-J.; Yu, S.-M. A Novel Class of Gibberellin 2-Oxidases Control Semidwarfism, Tillering, and Root Development in Rice. *Plant Cell* **2008**, *20*, 2603–2618. [[CrossRef](#)]
31. Zhang, Q.; Xie, J.; Zhu, X.; Ma, X.; Yang, T.; Khan, N.U.; Zhang, S.; Liu, M.; Li, L.; Liang, Y.; et al. Natural variation in Tiller Number 1 affects its interaction with TIF1 to regulate tillering in rice. *Plant Biotechnol. J.* **2023**, *21*, 1044–1057. [[CrossRef](#)]

32. Yang, Y.; Guo, Y. Unraveling salt stress signaling in plants. *J. Integr. Plant Biol.* **2018**, *60*, 796–804. [[CrossRef](#)]
33. Flowers, T.J.; Munns, R.; Colmer, T.D. Sodium chloride toxicity and the cellular basis of salt tolerance in halophytes. *Ann. Bot.* **2014**, *115*, 419–431. [[CrossRef](#)]
34. van Zelm, E.; Zhang, Y.; Testerink, C. Salt Tolerance Mechanisms of Plants. *Annu. Rev. Plant Biol.* **2020**, *71*, 403–433. [[CrossRef](#)]
35. Liu, C.; Mao, B.; Yuan, D.; Chu, C.; Duan, M. Salt tolerance in rice: Physiological responses and molecular mechanisms. *Crop J.* **2022**, *10*, 13–15. [[CrossRef](#)]
36. Zhao, C.; Zhang, H.; Song, C.; Zhu, J.-K.; Shabala, S. Mechanisms of Plant Responses and Adaptation to Soil Salinity. *Innovation* **2020**, *1*, 100017. [[CrossRef](#)]
37. Sanchez, D.H.; Siahpoosh, M.R.; Roessner, U.; Udvardi, M.; Kopka, J. Plant metabolomics reveals conserved and divergent metabolic responses to salinity. *Physiol. Plant.* **2007**, *132*, 209–219. [[CrossRef](#)] [[PubMed](#)]
38. Zhang, L.; Ma, B.; Wang, C.; Chen, X.; Ruan, Y.-L.; Yuan, Y.; Ma, F.; Li, M. MdWRKY126 modulates malate accumulation in apple fruit by regulating cytosolic malate dehydrogenase (MdMDH5). *Plant Physiol.* **2022**, *188*, 2059–2072. [[CrossRef](#)]
39. Ding, Z.J.; Yan, J.Y.; Xu, X.Y.; Li, G.X.; Zheng, S.J. WRKY46 functions as a transcriptional repressor of ALMT1, regulating aluminum-induced malate secretion in Arabidopsis. *Plant J.* **2013**, *76*, 825–835. [[CrossRef](#)]
40. Wang, Q.; Sun, H.; Dong, Q.; Sun, T.; Jin, Z.; Hao, Y.; Yao, Y. The enhancement of tolerance to salt and cold stresses by modifying the redox state and salicylic acid content via the cytosolic malate dehydrogenase gene in transgenic apple plants. *Plant Biotechnol. J.* **2016**, *14*, 1986–1997. [[CrossRef](#)] [[PubMed](#)]
41. Kandoi, D.; Mohanty, S.; Tripathy, B.C. Overexpression of plastidic maize NADP-malate dehydrogenase (ZmNADP-MDH) in Arabidopsis thaliana confers tolerance to salt stress. *Protoplasma* **2017**, *255*, 547–563. [[CrossRef](#)] [[PubMed](#)]
42. Etienne, A.; Génard, M.; Lobit, P.; Mbéguié-A-Mbéguié, D.; Bugaud, C. What controls fleshy fruit acidity? A review of malate and citrate accumulation in fruit cells. *J. Exp. Bot.* **2013**, *64*, 1451–1469. [[CrossRef](#)]
43. Beeler, S.; Liu, H.-C.; Stadler, M.; Schreier, T.; Eicke, S.; Lue, W.-L.; Truernit, E.; Zeeman, S.C.; Chen, J.; Kötting, O. Plastidial NAD-Dependent Malate Dehydrogenase Is Critical for Embryo Development and Heterotrophic Metabolism in Arabidopsis. *Plant Physiol.* **2014**, *164*, 1175–1190. [[CrossRef](#)]
44. Alabd, A.; Cheng, H.; Ahmad, M.; Wu, X.; Peng, L.; Wang, L.; Yang, S.; Bai, S.; Ni, J.; Teng, Y. ABRE-BINDING FACTOR3-WRKY DNA-BINDING PROTEIN44 module promotes salinity-induced malate accumulation in pear. *Plant Physiol.* **2023**, *192*, 1982–1996. [[CrossRef](#)]
45. Hu, D.-G.; Sun, C.-H.; Sun, M.-H.; Hao, Y.-J. MdSOS2L1 phosphorylates MdVHA-B1 to modulate malate accumulation in response to salinity in apple. *Plant Cell Rep.* **2015**, *35*, 705–718. [[CrossRef](#)]
46. Sweetman, C.; Deluc, L.G.; Cramer, G.R.; Ford, C.M.; Soole, K.L. Regulation of malate metabolism in grape berry and other developing fruits. *Phytochemistry* **2009**, *70*, 1329–1344. [[CrossRef](#)]
47. Wang, C.-R.; Li, X.-Y.; Yao, Y.-X.; Hao, Y.-J. Modifications of Kyoho grape berry quality under long-term NaCl treatment. *Food Chem.* **2013**, *139*, 931–937. [[CrossRef](#)]
48. Zhang, Y.; Wang, Y.; Sun, X.; Yuan, J.; Zhao, Z.; Gao, J.; Wen, X.; Tang, F.; Kang, M.; Abliz, B.; et al. Genome-Wide Identification of MDH Family Genes and Their Association with Salt Tolerance in Rice. *Plants* **2022**, *11*, 1498. [[CrossRef](#)]
49. de la Torre-González, A.; Albacete, A.; Sánchez, E.; Blasco, B.; Ruiz, J.M. Comparative study of the toxic effect of salinity in different genotypes of tomato plants: Carboxylates metabolism. *Sci. Hortic.* **2017**, *217*, 173–178. [[CrossRef](#)]
50. Yao, Y.-X.; Dong, Q.-L.; Zhai, H.; You, C.-X.; Hao, Y.-J. The functions of an apple cytosolic malate dehydrogenase gene in growth and tolerance to cold and salt stresses. *Plant Physiol. Biochem.* **2011**, *49*, 257–264. [[CrossRef](#)] [[PubMed](#)]
51. Scheibe, R. Malate valves to balance cellular energy supply. *Physiol. Plant.* **2004**, *120*, 21–26. [[CrossRef](#)] [[PubMed](#)]
52. Taniguchi, M.; Miyake, H. Redox-shuttling between chloroplast and cytosol: Integration of intra-chloroplast and extra-chloroplast metabolism. *Curr. Opin. Plant Biol.* **2012**, *15*, 252–260. [[CrossRef](#)]
53. Ma, B.; Yuan, Y.; Gao, M.; Xing, L.; Li, C.; Li, M.; Ma, F. Genome-wide Identification, Classification, Molecular Evolution and Expression Analysis of Malate Dehydrogenases in Apple. *Int. J. Mol. Sci.* **2018**, *19*, 3312. [[CrossRef](#)]
54. Lin, Y.; Chen, W.; Yang, Q.; Zhang, Y.; Ma, X.; Li, M. Genome-Wide Characterization and Gene Expression Analyses of Malate Dehydrogenase (MDH) Genes in Low-Phosphorus Stress Tolerance of Chinese Fir (*Cunninghamia lanceolata*). *Int. J. Mol. Sci.* **2023**, *24*, 4414. [[CrossRef](#)]
55. Imran, M.; Tang, K.; Liu, J.-Y. Comparative Genome-Wide Analysis of the Malate Dehydrogenase Gene Families in Cotton. *PLoS ONE* **2016**, *11*, e0166341. [[CrossRef](#)]
56. Menckhoff, L.; Mielke-Ehret, N.; Buck, F.; Vuletić, M.; Lüthje, S. Plasma membrane-associated malate dehydrogenase of maize (*Zea mays* L.) roots: Native versus recombinant protein. *J. Proteom.* **2013**, *80*, 66–77. [[CrossRef](#)]
57. Lü, G.; Liang, Y.; Wu, X.; Li, J.; Ma, W.; Zhang, Y.; Gao, H. Molecular cloning and functional characterization of mitochondrial malate dehydrogenase (mMDH) is involved in exogenous GABA increasing root hypoxia tolerance in muskmelon plants. *Sci. Hortic.* **2019**, *258*, 108741. [[CrossRef](#)]
58. Chen, X.; Zhang, J.; Zhang, C.; Wang, S.; Yang, M. Genome-wide investigation of malate dehydrogenase gene family in poplar (*Populus trichocarpa*) and their expression analysis under salt stress. *Acta Physiol. Plant.* **2021**, *43*, 1–10. [[CrossRef](#)]
59. Lü, J.; Gao, X.; Dong, Z.; Yi, J.; An, L. Improved phosphorus acquisition by tobacco through transgenic expression of mitochondrial malate dehydrogenase from *Penicillium oxalicum*. *Plant Cell Rep.* **2011**, *31*, 49–56. [[CrossRef](#)] [[PubMed](#)]

60. Imran, M.; Munir, M.Z.; Ialhi, S.; Abbas, F.; Younus, M.; Ahmad, S.; Naeem, M.K.; Waseem, M.; Iqbal, A.; Gul, S.; et al. Identification and Characterization of Malate Dehydrogenases in Tomato (*Solanum lycopersicum* L.). *Int. J. Mol. Sci.* **2022**, *23*, 10028. [[CrossRef](#)]
61. Zhu, S.; Chen, Z.; Xie, B.; Guo, Q.; Chen, M.; Liang, C.; Bai, Z.; Wang, X.; Wang, H.; Liao, H.; et al. A phosphate starvation responsive malate dehydrogenase, GmMDH12 mediates malate synthesis and nodule size in soybean (*Glycine max*). *Environ. Exp. Bot.* **2021**, *189*, 104560. [[CrossRef](#)]
62. Liu, T.; Zhang, X.; Zhang, H.; Cheng, Z.; Liu, J.; Zhou, C.; Luo, S.; Luo, W.; Li, S.; Xing, X.; et al. Dwarf and High Tillering1 represses rice tillering through mediating the splicing of D14 pre-mRNA. *Plant Cell* **2022**, *34*, 3301–3318. [[CrossRef](#)]
63. Chen, Y.; Fu, Z.; Zhang, H.; Tian, R.; Yang, H.; Sun, C.; Wang, L.; Zhang, W.; Guo, Z.; Zhang, X.; et al. Cytosolic malate dehydrogenase 4 modulates cellular energetics and storage reserve accumulation in maize endosperm. *Plant Biotechnol. J.* **2020**, *18*, 2420–2435. [[CrossRef](#)]
64. Wang, Z.-A.; Li, Q.; Ge, X.-Y.; Yang, C.-L.; Luo, X.-L.; Zhang, A.-H.; Xiao, J.-L.; Tian, Y.-C.; Xia, G.-X.; Chen, X.-Y.; et al. The mitochondrial malate dehydrogenase 1 gene GmMDH1 is involved in plant and root growth under phosphorus deficiency conditions in cotton. *Sci. Rep.* **2015**, *5*, 10343. [[CrossRef](#)] [[PubMed](#)]
65. Nan, N.; Wang, J.; Shi, Y.; Qian, Y.; Jiang, L.; Huang, S.; Liu, Y.; Wu, Y.; Liu, B.; Xu, Z. Rice plastidial NAD-dependent malate dehydrogenase 1 negatively regulates salt stress response by reducing the vitamin B6 content. *Plant Biotechnol. J.* **2019**, *18*, 172–184. [[CrossRef](#)]
66. Teng, X.; Zhong, M.; Zhu, X.; Wang, C.; Ren, Y.; Wang, Y.; Zhang, H.; Jiang, L.; Wang, D.; Hao, Y.; et al. FLOURY ENDOSPERM16 encoding a NAD-dependent cytosolic malate dehydrogenase plays an important role in starch synthesis and seed development in rice. *Plant Biotechnol. J.* **2019**, *17*, 1914–1927. [[CrossRef](#)]
67. Pracharoenwattana, I.; Cornah, J.E.; Smith, S.M. Arabidopsis peroxisomal malate dehydrogenase functions in β -oxidation but not in the glyoxylate cycle. *Plant J.* **2007**, *50*, 381–390. [[CrossRef](#)] [[PubMed](#)]
68. Nozoye, T.; Nagasaka, S.; Kobayashi, T.; Sato, Y.; Uozumi, N.; Nakanishi, H.; Nishizawa, N.K. The Phytosiderophore Efflux Transporter TOM2 Is Involved in Metal Transport in Rice. *J. Biol. Chem.* **2015**, *290*, 27688–27699. [[CrossRef](#)]
69. Zhao, L.; Tan, L.; Zhu, Z.; Xiao, L.; Xie, D.; Sun, C. PAY1 improves plant architecture and enhances grain yield in rice. *Plant J.* **2015**, *83*, 528–536. [[CrossRef](#)]
70. Tomaz, T.; Bagard, M.; Pracharoenwattana, I.; Lindén, P.; Lee, C.P.; Carroll, A.J.; Ströher, E.; Smith, S.M.; Gardeström, P.; Millar, A.H. Mitochondrial Malate Dehydrogenase Lowers Leaf Respiration and Alters Photorespiration and Plant Growth in Arabidopsis. *Plant Physiol.* **2010**, *154*, 1143–1157. [[CrossRef](#)] [[PubMed](#)]
71. Selinski, J.; König, N.; Wellmeyer, B.; Hanke, G.T.; Linke, V.; Neuhaus, H.E.; Scheibe, R. The Plastid-Localized NAD-Dependent Malate Dehydrogenase Is Crucial for Energy Homeostasis in Developing Arabidopsis thaliana Seeds. *Mol. Plant* **2014**, *7*, 170–186. [[CrossRef](#)]
72. Liu, L.; Ren, M.; Peng, P.; Chun, Y.; Li, L.; Zhao, J.; Fang, J.; Peng, L.; Yan, J.; Chu, J.; et al. MIT1, encoding a 15-cis- ζ -carotene isomerase, regulates tiller number and stature in rice. *J. Genet. Genom.* **2021**, *48*, 88–91. [[CrossRef](#)]
73. Jin, C.; Sun, Y.; Shi, Y.; Zhang, Y.; Chen, K.; Li, Y.; Liu, G.; Yao, F.; Cheng, D.; Li, J.; et al. Branched-chain amino acids regulate plant growth by affecting the homeostasis of mineral elements in rice. *Sci. China Life Sci.* **2019**, *62*, 1107–1110. [[CrossRef](#)] [[PubMed](#)]
74. Bashir, K.; Inoue, H.; Nagasaka, S.; Takahashi, M.; Nakanishi, H.; Mori, S.; Nishizawa, N.K. Cloning and Characterization of Deoxymugineic Acid Synthase Genes from Gramineous. *Plants J. Biol. Chem.* **2006**, *281*, 32395–32402. [[CrossRef](#)]
75. Jia, M.; Luo, N.; Meng, X.; Song, X.; Jing, Y.; Kou, L.; Liu, G.; Huang, X.; Wang, Y.; Li, J.; et al. OsMPK4 promotes phosphorylation and degradation of IPA1 in response to salt stress to confer salt tolerance in rice. *J. Genet. Genom.* **2022**, *49*, 766–775. [[CrossRef](#)]
76. Wu, Z.; Guo, Z.; Wang, K.; Wang, R.; Fang, C. Comparative Metabolomic Analysis Reveals the Role of OsHPL1 in the Cold-Induced Metabolic Changes in Rice. *Plants* **2023**, *12*, 2032. [[CrossRef](#)] [[PubMed](#)]
77. Sun, Y.; Wang, B.; Ren, J.; Zhou, Y.; Han, Y.; Niu, S.; Zhang, Y.; Shi, Y.; Zhou, J.; Yang, C.; et al. OsbZIP18, a Positive Regulator of Serotonin Biosynthesis, Negatively Controls the UV-B Tolerance in Rice. *Int. J. Mol. Sci.* **2022**, *23*, 3215. [[CrossRef](#)] [[PubMed](#)]
78. Zhang, Y.; Chen, K.; Zhao, F.-J.; Sun, C.; Jin, C.; Shi, Y.; Sun, Y.; Li, Y.; Yang, M.; Jing, X.; et al. OsATX1 Interacts with Heavy Metal P1B-Type ATPases and Affects Copper Transport and Distribution. *Plant Physiol.* **2018**, *178*, 329–344. [[CrossRef](#)] [[PubMed](#)]

Disclaimer/Publisher's Note: The statements, opinions and data contained in all publications are solely those of the individual author(s) and contributor(s) and not of MDPI and/or the editor(s). MDPI and/or the editor(s) disclaim responsibility for any injury to people or property resulting from any ideas, methods, instructions or products referred to in the content.